CARBON 91 (2015) 76–87

Available at www.sciencedirect.com

ScienceDirect

journal homepage: www.elsevier.com/locate/carbon

Dielectric constant and electrical conductivity of carbon black as an electrically conductive additive in a manganese-dioxide electrochemical electrode, and their dependence on electrolyte permeation

Morteza Moalleminejad, D.D.L. Chung *

Composite Materials Research Laboratory, University at Buffalo, State University of New York, Buffalo, NY 14260-4400, USA

ARTICLE INFO

Article history:
Received 29 January 2015
Accepted 17 April 2015
Available online 24 April 2015

ABSTRACT

The relative dielectric constant and electrical conductivity of electrochemical electrodes with manganese-dioxide (MnO_2) particles mixed with carbon black (CB, the most common electrically conductive additive) are reported, with unprecedented determination of the decoupled CB properties and their dependence on the MnO_2 volume fraction. The electrolyte is 15 vol.% sulfuric acid. As the CB proportion increases, the CB electrical conduction connectivity increases, while the CB dielectric connectivity decreases (due to decreasing squishing by the MnO_2). The minimum MnO_2 content for squishing the CB to the extent of enhancing the CB polarizability is 65 vol.%. The electrolyte enhances the CB conduction/dielectric connectivity. Without electrolyte permeation, as the CB proportion increases from 14 to 30 vol.% (the MnO_2 proportion correspondingly decreasing from 69 to 59 vol.%), the CB resistivity decreases from 236 to 165 Ω cm and the CB relative dielectric constant decreases from 53 to 12 (leveling-off below 65 vol.% MnO_2), suggesting decreasing CB polarizability as CB is less squished. With complete electrolyte permeation, as the CB proportion increases from 18 to 25 vol.%, the CB resistivity decreases from 49 to 34 Ω cm and the CB relative dielectric constant decreases from 29 to 22. Without MnO_2, the CB conduction connectivity is the highest.

1. Introduction

Manganese dioxide (MnO_2) is a widely used active electrochemical electrode material that is used in the form of particles [1], with major applications including dry-cell batteries, such as the alkaline battery and the zinc–carbon battery [2,3]. In the alkaline battery, zinc is the anode while MnO_2 is the cathode; both the anode and the cathode are in the form of electrolyte-based particle pastes. In addition, MnO_2 is used as electrodes in supercapacitors in the form of pseudocapacitors [4–15]. In the pseudocapacitor, sulfuric acid is often used as the electrolyte to provide H^+ ions (protons), which react with the MnO_2 to cause the reduction of MnO_2 during charging; the opposite reaction (oxidation) occurs during discharging.

Due to its inadequate electrical conductivity, MnO_2 is commonly mixed with a conductive additive. The most common

* *Corresponding author:* Fax: +1 (716) 645 2883.
E-mail address: ddlchung@buffalo.edu (D.D.L. Chung).
URL: http://alum.mit.edu/www/ddlchung (D.D.L. Chung).
http://dx.doi.org/10.1016/j.carbon.2015.04.047
0008-6223/

conductive additive used in practice is carbon black (CB) [16–20], although graphene, graphene oxide and carbon nanotubes are starting to be used [21–27].

The CB is attractive for its low cost, squishability and long history of effective use as a conductive additive. The squishability refers to its extensive compressibility, which results from the fact that carbon black is in the form of porous aggregates of nanoparticles. Due to the squishability, CB spreads upon being compressed between the MnO_2 particles, thereby promoting the electrical connectivity of the CB amidst the MnO_2 particles. In contrast, carbon nanofiber (CNF, originally known as carbon filament) is not squishable. Thus, in spite of its large aspect ratio, CNF (particularly if it is not graphitized) is not as effective as CB for enhancing the conductivity of an MnO_2 electrode [3,28], even though it is more effective than CB for providing a conductive carbon compact in the absence of MnO_2 particles [3]. The electrical resistivity of a dry compact of MnO_2 particles and CNF (16.6 vol.%) is down to 8 Ω cm, whereas that of a dry compact of MnO_2 particles and CB (15.2 vol.%) is down to 3 Ω cm [3]. In contrast, the resistivity of a dry compact of CNF (without MnO_2) is down to 0.020 Ω cm, whereas that of a dry compact of CB (without MnO_2) is down to 0.046 Ω cm [25]. The presence of the stiff MnO_2 particles facilitates the squishing of the CB located between the particles, thereby causing the CB to be highly effective (even more effective than CNF) for enhancing the conductivity. Without the MnO_2 particles, the squishing of the CB is less, so that the CB becomes less effective than CNF for providing low resistivity. The CB is also more effective than natural graphite and graphitized mesophase pitch for enhancing the conductivity of an MnO_2 electrode [28].

A high value of the relative dielectric constant (i.e., the real part of the relative permittivity) is desired for the electrolyte and the electrodes of a supercapacitor (double-layer capacitor). In contrast, for a battery, a low value of the relative dielectric constant is desired for the electrodes, as electric polarization in an electrode is disadvantageous to battery performance. Low values of the volume resistivity of the electrolyte and electrodes are desired for both supercapacitors and batteries in order to minimize the internal resistance of the electrochemical cell. In particular, a low volume resistivity of the electrode helps the transmission of the applied electric potential from the electrical contact to the electrode–electrolyte interface.

Prior work on electrodes of MnO_2 with carbon has emphasized testing in the electrochemical cell level, using techniques such as cyclic voltammetry, charge–discharge testing and electrochemical impedance spectroscopy [16–27,3], with little attention on testing in the material level [3,28]. The cell-level testing does not allow decoupling of the contributions by the cell components, such as the electrodes and the electrolyte. As a consequence, it is commonly assumed that MnO_2 is completely non-conductive, while the carbon is conductive, with negligible polarizability. For rigorous understanding of cell behavior and precise design of electrochemical cells, it is important to go beyond this assumption by determining the electrical conductivity and relative dielectric constant of each component of the electrode (MnO_2 and carbon). Both the dielectric behavior and the conduction behavior are important for understanding cell performance. The information is valuable for guiding electrode and cell design.

Although prior work has been directed at studying either the electrochemical cells with a combination of MnO_2 and carbon as an electrode [16–27,3] or the MnO_2–carbon electrode by itself, it provides information on the cell or electrode performance without decoupling the contributions of MnO_2 and carbon to the cell or electrode behavior. Due to the squishing of the CB in the presence of MnO_2 [3], the structure of the CB is expected to be affected by the presence of MnO_2. Without the decoupling, the structure and associated properties of the CB cannot be effectively studied. This work provides this decoupling for the first time.

Prior work has reported the electrical resistivity of dry (without an electrolyte) MnO_2–CB compacts [3,28] and the relative dielectric constant and electrical resistivity of dry CB compacts (without MnO_2) [29], and CB electrolyte-based pastes (without MnO_2) [29], with the electrolyte being 15 vol.% sulfuric acid. With the goal of studying the behavior of the CB in an MnO_2 electrode, this work addresses systematically dry MnO_2 compacts (without CB), dry MnO_2–CB compacts, MnO_2 electrolyte-based pastes (without CB) and MnO_2–CB electrolyte-based pastes.

This work is mainly directed at studying the resistivity and relative dielectric constant of the CB in an MnO_2 paste electrode with the liquid in the paste being the electrolyte and with various proportions of MnO_2 and CB in the paste. A fundamental scientific question addressed in this paper relates to the effects of the presence and volume fraction of the MnO_2 on the structure and properties of the CB in the electrode.

2. Experimental and analytical methods

The approach used for achieving the decoupling mentioned in Section 1 involves measuring the resistance and capacitance of (i) the dry MnO_2 and MnO_2–CB compacts (for determining the quantities pertaining to the MnO_2 and CB in the absence of an electrolyte), (ii) an electrolyte-containing paper towel (for determining the quantities pertaining to the electrolyte), and (iii) the MnO_2 and MnO_2–CB electrolyte-based pastes (for determining the quantities pertaining to the MnO_2 and CB in the presence of the electrolyte). The measurement of each property is conducted for three specimen thicknesses, thereby decoupling specimen volumetric and specimen-contact interfacial quantities (Fig. 1). The contact refers to the electrical contact to the electrode.

This approach was previously used to study carbon (without MnO_2) electrodes [29]. However, this approach has not been previously used to study MnO_2 electrodes, whether with or without carbon. The value of this approach relates to its ability to decouple the volumetric and interfacial quantities and to decouple the contributions from the various constituents in the electrode. Prior to Ref. 29, work on carbon, MnO_2 or other electrode materials measured the capacitance with the volumetric and interfacial contributions as a lumped quantity, without decoupling. In other words, the prior work assumed that the interfacial contribution is negligible.

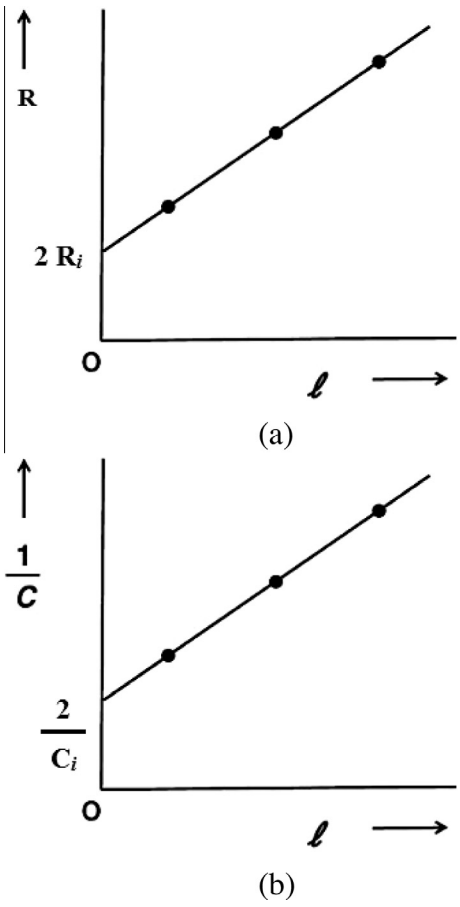

Fig. 1 – Schematic plots. In the horizontal axis, *l* is the thickness of the specimen. (a) Plot of resistance *R* vs. thickness *l* for the determination of specimen-contact interfacial resistance R_i and volumetric specimen resistance R_s. The slope equals the volumetric specimen resistance R_s per unit thickness. The intercept on the vertical axis equals $2R_i$. (b) Plot of the reciprocal of the capacitance *C* vs. thickness *l*, for the determination of the specimen-contact interfacial capacitance C_i and the specimen relative dielectric constant κ. The slope equals $1/(\varepsilon_0 \kappa A)$, where *A* is the specimen area and ε_0 is the permittivity of free space. The intercept on the vertical axis equals $2/C_i$.

This work uses equivalent circuit models to decouple the contributions from the various constituents, i.e., MnO_2, CB and electrolyte/air. In this work, compacts refer to the case without any electrolyte permeation (i.e., with air voids), whereas pastes refer to the case with complete electrolyte permeation (i.e., with the electrolyte replacing the air). Fig. 2 shows the equivalent circuit models for (a) the MnO_2 compact, (b) the MnO_2–CB compact, (c) the MnO_2 paste, and (d) the MnO_2–CBMnO_2–CB paste. All the quantities shown in the model have been decoupled. The quantities for CB in the absence of MnO_2 have been determined in prior work [29]. The contribution of the MnO_2-electrolyte interface is not included in Fig. 2, because it is found to be negligible through the decoupling. The basis for the circuit models and the method of decoupling are explained in Sections 2.2 and 2.3.

2.1. Materials

The MnO_2 exhibits the rutile crystal structure. It is a black powder that is insoluble in water. The typical particle size is 0.90 μm, as shown by microscopy. It is supplied by Fisher Scientific (Product S93297), with specific gravity 5.02 (close to the theoretical value of 5.026 for MnO_2), and containing MnO_2 (82–85 wt.%), quartz (1–3 wt.%) and barium compounds (1–2 wt.%). The material is derived from natural pyrolusite ore (specific gravity about 4.8). Pyrolusite is a mineral consisting essentially of MnO_2 and having density lower than that of MnO_2.

The carbon black (Ketjenblack EC600JD) is a furnace black from Akzo Nobel, Chicago, IL, USA). It has specific surface area 1236 ± 47 m^2/g and density 1.80 g/cm^3.

In relation to the case without any electrolyte permeation, mixtures consisting of MnO_2 and CB at various mass ratios of MnO_2 to CB are prepared by manual mixing. Then each mixture at a controlled mass is used to fill the cavity defined by the flexible graphite frame depicted in Fig. 3. Subsequently, the mixture in the cavity is manually compacted using a matching piston. A similar procedure is used when CB is not used, though the mixing step is obviously not needed.

In relation to the case with complete electrolyte permeation, a paste consisting of MnO_2 particles, CB and an aqueous liquid electrolyte (15 vol.% sulfuric acid) is prepared by mixing of known masses of the solid and liquid using a magnetic stirrer, followed by centrifuging for 10 h, which results in a liquid above a paste. The centrifuging step eliminates air from the resulting paste. This liquid is decanted and weighed. The paste is then heated at 80 °C for 5.5 h in order to allow a part of the liquid to evaporate. The mass ratio and hence the volume ratio of the solid and liquid parts of the paste are obtained. A similar procedure is used when CB is not used, though the mixing step is obviously not needed. Thus, paste A (without CB) containing 82.7 ± 2.2 vol.% MnO_2 and 17.3 ± 1.4 vol.% electrolyte, paste B (with CB) containing 64.6 ± 2.0 vol.% MnO_2, 18.1 ± 0.9 vol.% CB, and 17.3 ± 0.9 vol.% electrolyte, and paste C (with CB) containing 58.3 ± 1.8 vol.% MnO_2, 24.5 ± 1.0 vol.% CB, and 17.2 ± 0.9 vol.% electrolyte are obtained. The proportion of CB relative to MnO_2 is greater for paste C than paste B. The electrolyte volume fraction (about 17.3%) is similar for the three pastes, so that comparison of the three pastes for studying the effect of the CB volume fraction is meaningful.

2.2. Approach

2.2.1. Compacts

The measured values of the relative dielectric constant and resistivity of an MnO_2 compact (without CB) are used to calculate the corresponding values of the MnO_2 in the compact, based on the equivalent circuit model with MnO_2 and air in parallel (Fig. 2(a)). With these values for MnO_2 and the measured values of an MnO_2–CB compact, the values for the CB in the compact are calculated, based on an equivalent circuit model with MnO_2, CB and air in parallel (Fig. 2(b)).

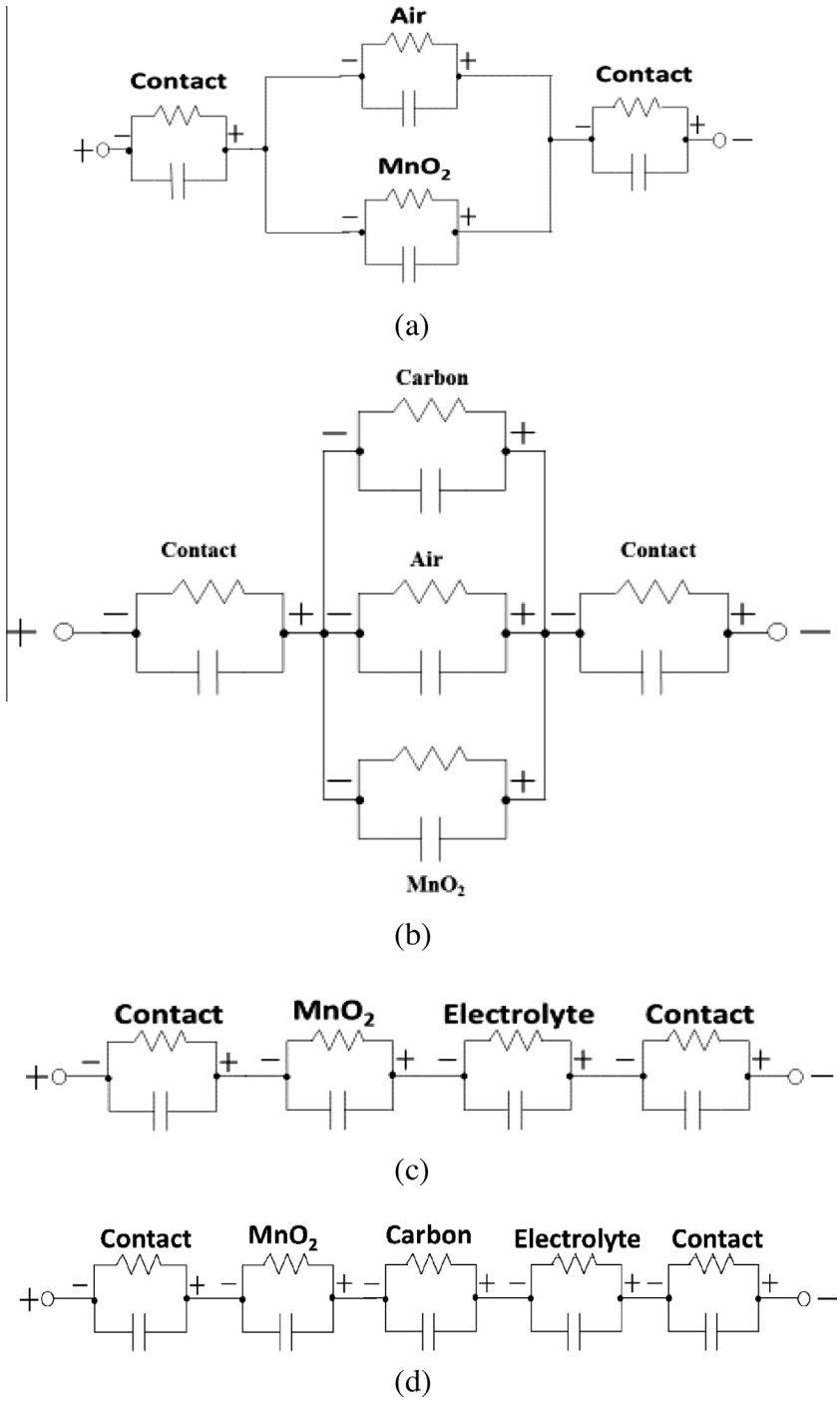

Fig. 2 – Equivalent circuit models for (a) MnO_2 compact (without CB), (b) MnO_2–CB compact, (c) MnO_2 paste (without CB), (d) MnO_2–CB paste. The contact refers to the interface between the compact/paste and the electrical contact.

2.2.2. Pastes

Information on the properties of the electrolyte allows the contribution of the electrolyte to the measured properties to be decoupled from the contributions from MnO_2 and CB. The relative dielectric constant and resistivity of the electrolyte (after heating at 80 °C for 5.5 h) are separately measured following the method (involving paper towel soaked with the electrolyte) of prior work [29]. The previously reported values [29] are for the electrolyte without heating. The relative dielectric constant of the electrolyte after the heating, which is for evaporating away a part of the electrolyte in the paste, is 112.0 ± 1.8 (higher than the value of 100.9 ± 1.3 for the electrolyte without heating [29]). The resistivity of the electrolyte after the heating is 3.8 ± 0.6 Ω cm (lower than the value of 5.7 ± 1.2 Ω cm for the electrolyte without heating [29]). The heating causes evaporation, such that the ion concentration (such as the H^+ concentration due to the sulfuric acid) is increased, thereby increasing the relative dielectric constant and decreasing the resistivity. These value for the electrolyte are considered to be not affected by the

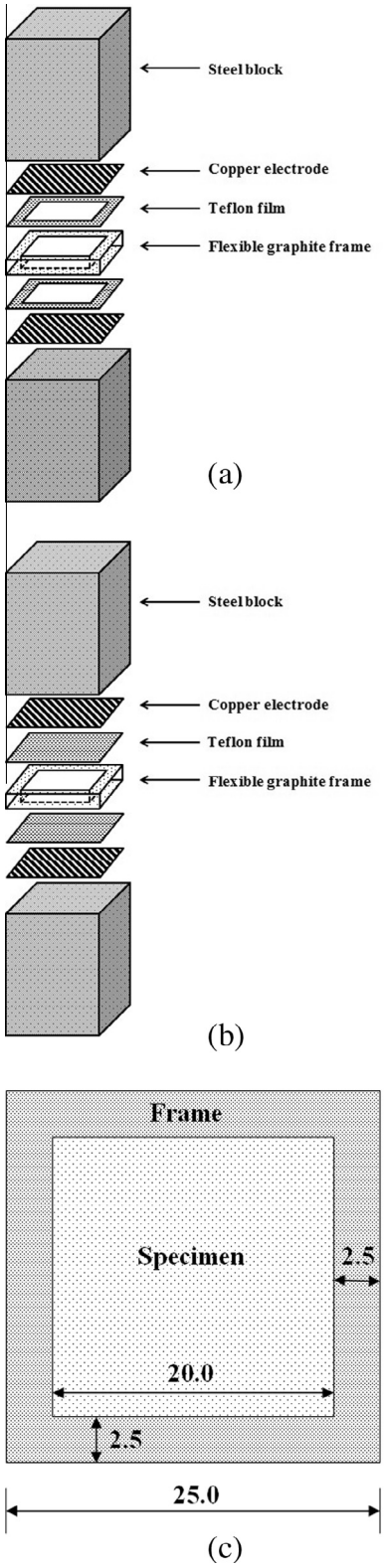

Fig. 3 – Configuration for resistive and dielectric testing. (a) Side view of the configuration for electrical resistance measurement. (b) Side view of the configuration for dielectric measurement. (c) Top view of the configuration for either resistance or dielectric measurement. All dimensions are in mm.

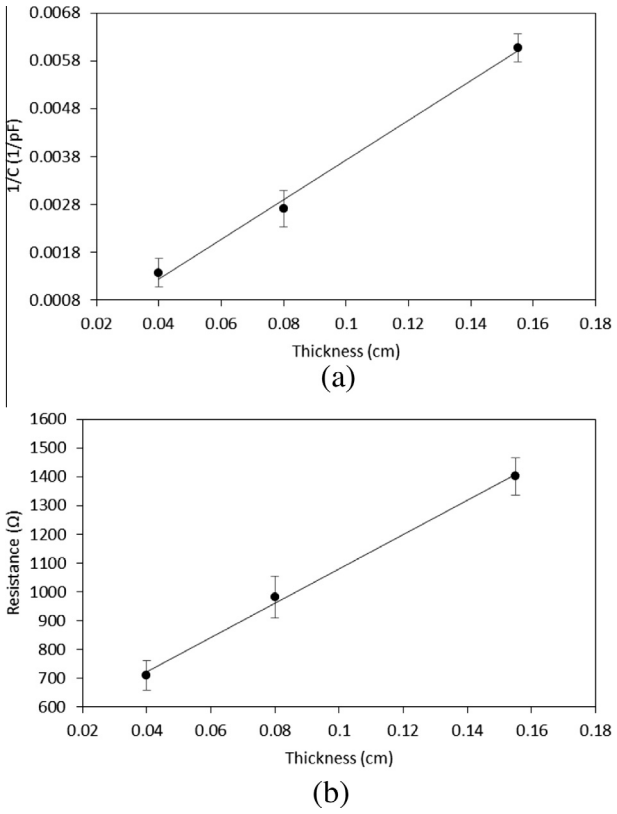

Fig. 4 – Representative plots for a compact containing 65 vol.% MnO_2 and 19 vol.% carbon black. (a) Plot of 1/C (the reciprocal of the capacitance) vs. thickness, with the slope of the plot related to the relative dielectric constant of the specimen. (b) Plot of resistance vs. thickness, with the slope of the plot related to the resistivity of the specimen.

presence of MnO_2 or CB, as supported by prior work involving carbon particle pastes [29]. The determination of the electrolyte properties are described in detail in the Supplementary material section.

With the values of the relative dielectric constant and resistivity of the electrolyte, the measured values of the relative dielectric constant and resistivity of paste A (without CB) are used to calculate the corresponding values of the MnO_2 in the paste, based on the equivalent circuit model with MnO_2 and the electrolyte in series (Fig. 2(c)). Using these values of the MnO_2 and the electrolyte, the measured values of the relative dielectric constant and resistivity of paste B/C (with CB) are used to calculate the corresponding value of the CB in the paste, based on the equivalent circuit model with MnO_2, CB and the electrolyte in series (Fig. 2(d)).

2.3. *Dielectric testing and analysis method*

The measurement of the relative dielectric constant and the specific interfacial capacitance involves a precision RLC meter (Quadtech 7600). The frequency is 50 Hz. The capacitance for the parallel RC circuit configuration is obtained from the meter. The AC electric field is 6.5 V/cm. In order to decouple the volumetric and interfacial contributions to the capacitance,

Table 1 – Relative dielectric constant and resistivity of MnO_2–CB compacts and the CB part of the compact. CB = carbon black. Relative dielectric constant of MnO_2 = 68.1 ± 1.6, and resistivity of MnO_2 = 8790 ± 280 Ω cm, as obtained for the MnO_2 compact without CB (using the equivalent circuit in Fig. 2(a)) and considered to be unaffected by the CB addition. The compacts containing CB are analyzed using the equivalent circuit model in Fig. 2(b).

CB/MnO_2 mass ratio (%)	Volume fraction (%)			Relative dielectric constant		Resistivity (Ω cm)	
	MnO_2	CB	Porosity	Compact	CB	Compact	CB
0	60.2 ± 1.0	0	39.8 ± 1.0	64.5 ± 0.8	/	14,648 ± 225	/
2.18 ± 0.01	68.6 ± 0.6	13.5 ± 1.2	18.0 ± 1.8	53.4 ± 0.8	52.5 ± 4.2	1498 ± 11	236 ± 4
5.04 ± 0.02	66.9 ± 2.2	14.8 ± 1.3	18.3 ± 3.5	53.4 ± 1.6	40.6 ± 1.5	1359 ± 7	219 ± 2
10.09 ± 0.01	64.5 ± 1.8	18.9 ± 1.2	16.6 ± 3.1	46.6 ± 2.3	20.1 ± 1.2	957 ± 6	200 ± 3
15.08 ± 0.01	58.7 ± 1.5	29.5 ± 2.4	13.4 ± 3.9	44.3 ± 1.7	12.3 ± 0.7	566 ± 6	165 ± 2

specimens of three different thicknesses (0.42, 1.60 and 3.30 mm) are tested (Fig. 3), as dictated by those of three frames (with through holes) made of flexible graphite (a sheet commercially made by the compression of exfoliated graphite in the absence of a binder), which is chosen for its chemical inertness and fluid gasketing ability. The electric field is applied between the two copper foils (Fig. 3). The AC voltage is adjusted so that the electric field is fixed while the thickness varies. Each specimen fills the entire volume (area 20.0 × 20.0 mm) inside a frame (outer dimensions 25.0 × 25.0 mm, Fig. 3(c)). For both dielectric and resistance measurements, the flexible graphite frame is insulated from each of the two copper contacts (copper foils of thickness 62 μm) by using a glass fiber fabric reinforced Teflon film (CS Hyde Company, Lake Villa, IL) of thickness 75 μm (Fig. 3). The pressure provided by a copper foil and a steel weight above it on the specimen during testing is 4.3 kPa (0.63 psi).

In case of dielectric measurement (Fig. 3(b)), the Teflon film with area 25.0 × 25.0 mm (covering both the specimen and the frame) and relative dielectric constant 2.34 (as measured at 1.000 kHz) is used as an insulating film between the specimen and each of the two copper contacts. In case of resistance measurement, this continuous film is replaced by a frame (with a square through-hole) made by using the same material and positioned between the specimen and the copper (Fig. 3(a)). Thus, the contact is copper in case of conduction testing and Teflon-lined copper in case of dielectric testing. The continuous Teflon lining used in dielectric testing is for minimizing the current.

The measured capacitance C is for the combination of the specimen and the frame in parallel electrically, with inclusion of the effect of the two interfaces between this combination and the two contacts. The two interfaces and this combination are in series electrically. Hence,

$$1/C = 2/C_i + l/(\varepsilon_0 \kappa A), \quad (1)$$

where C_i is the capacitance due to a combination-contact interface, ε_0 is the permittivity of free space (8.85×10^{-12} F/m), κ is the relative dielectric constant of the combination, A is the contact area, which is the same as the specimen area (20.0×20.0 mm^2), and l is the thickness of the frame. As shown by Eq. (1), C_i should be high in order for it to have little influence.

According to Eq. (1), 1/C is plotted against l, as illustrated in Fig. 1(b). The value of C_i is obtained from the intercept of $2/C_i$ at the $1/C$ axis at $l = 0$, and the value of κ is obtained from the slope, which is equal to $1/(\varepsilon_0 \kappa A)$.

The relative dielectric constant (κ) of the combination (specimen plus frame) is related to that of the specimen material κ_s and that of the frame material κ_r by the Rule of Mixtures, as shown by the equation

$$\kappa = \kappa_s v_s + \kappa_r v_r, \quad (2)$$

where v_s is the area fraction of the specimen, and v_r is the area fraction of the frame, with the two area fractions adding up to unity.

For an MnO_2 compact, the MnO_2, CB (if present) and air are considered as being in parallel (Fig. 2(a) and 2(b)). The capacitance of the compact C_c is thus related to the contributions by the MnO_2 (C_m), CB (C_b) and air (C_a) by the equation

$$C_c = C_m + C_b + C_a. \quad (3)$$

Based on Eq. (3), κ_c is given by

$$\kappa_c = V_m \kappa_m + V_b \kappa_b + (1 - V_m - V_b), \quad (4)$$

where κ_b is the relative dielectric constant of the CB, V_m is the volume fraction of the MnO_2 and V_b is the volume fraction of the CB. With κ_c measured and κ_m determined using Eq. (5) for the compact without CB (i.e., $V_b = 0$), κ_b is obtained using Eq. (4). In other words, κ_m is considered to be unaffected by the presence of the CB.

For an MnO_2 paste without CB, both the solid part (MnO_2) and the liquid part (the electrolyte) contribute to the relative dielectric constant of the paste κ_p. The capacitance of the paste C_p is related to the contributions by the MnO_2 (C_m) and the electrolyte (C_e), according to the Rule of Mixtures for capacitors in series, i.e.,

$$1/C_p = 1/C_m + 1/C_e. \quad (5)$$

The configuration of capacitors in series for MnO_2 and the electrolyte in the paste (Fig. 2(c)) is due to the invalidity of the parallel configuration when the resistivity is considered (Section 2.4). On the other hand, in relation to the relative dielectric constant, the parallel and series models give similar results for the solid part of the paste. Based on Eq. (5) and the Rule of Mixtures for capacitors in series, the relative dielectric constant κ_p of the paste is given by the equation

$$1/\kappa_p = V_m/\kappa_m + (1 - V_m)/\kappa_e, \quad (6)$$

where κ_m is the relative dielectric constant of the MnO_2 solid in the paste, κ_e is the relative dielectric constant of the

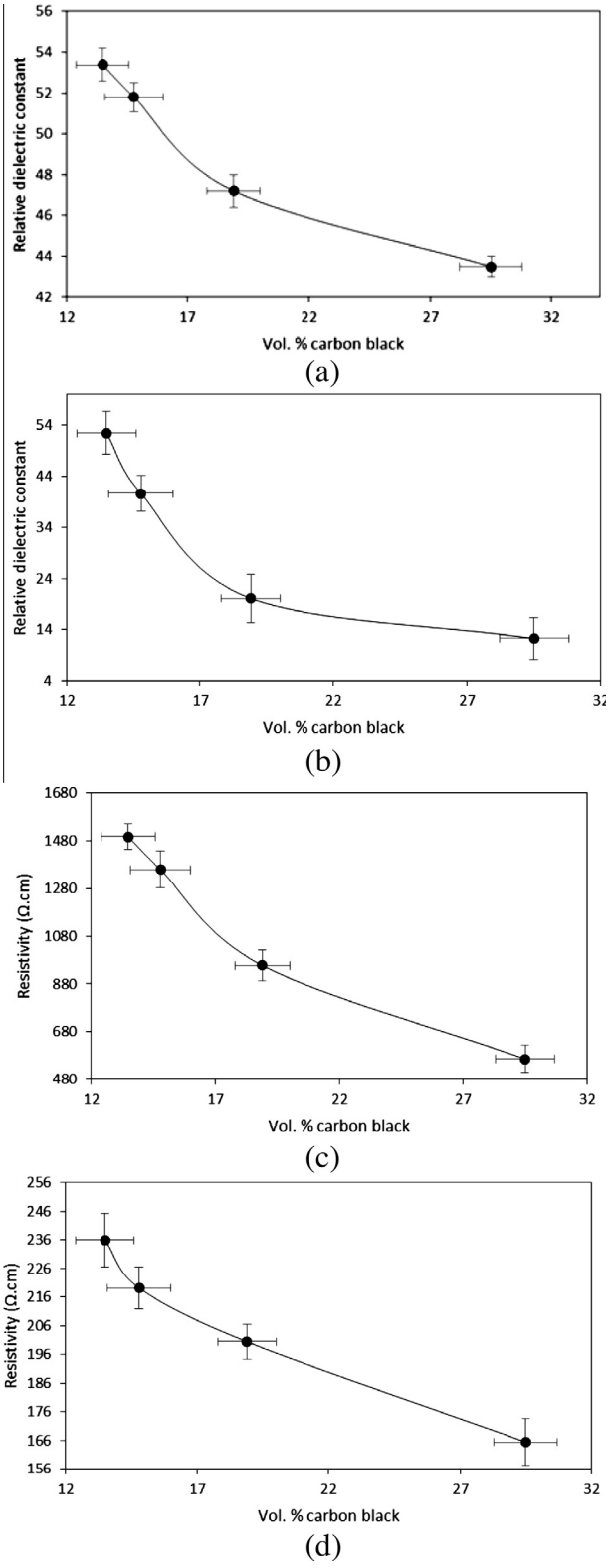

Fig. 5 – Effect of the volume fraction of carbon black (CB) on the relative dielectric constant and resistivity of MnO_2–CB compact and of the CB part of the compact. (a) Relative dielectric constant of the compact. (b) Relative dielectric constant of the CB in the compact. (c) Resistivity of the compact. (d) Resistivity of the CB in the compact.

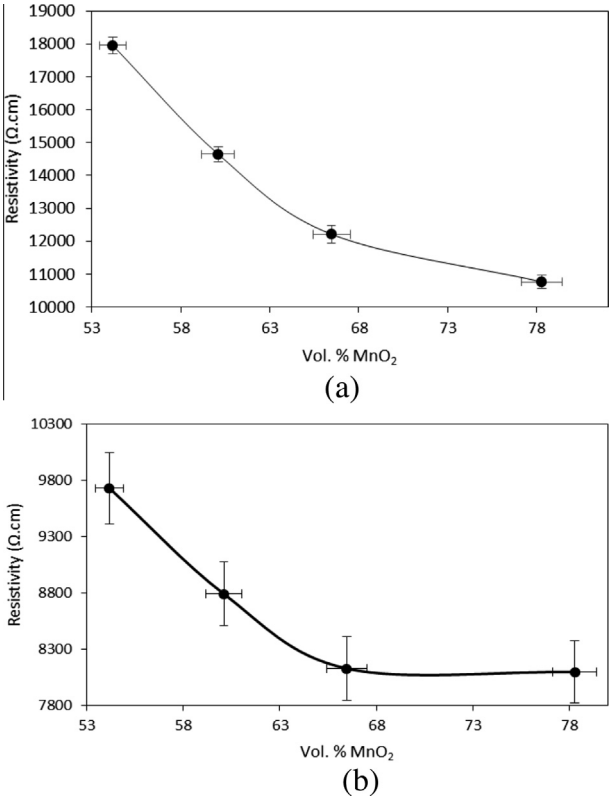

Fig. 6 – Effect of MnO_2 volume fraction on the electrical resistivity. (a) Resistivity of the MnO_2 compact (without CB). (b) Resistivity of the MnO_2 solid in the compact (without CB), as obtained from the resistivity of the MnO_2 compact by using the equivalent circuit in Fig. 2(a).

electrolyte, and V_m is the volume fraction of the MnO_2 in the paste. With κ_p measured, κ_m for MnO_2 in the presence of the electrolyte is obtained using Eq. (6).

For an MnO_2 paste with CB, the MnO_2, CB and electrolyte are considered as being in series (Fig. 2(d)). The capacitance of the paste C_p is thus related to the contributions by the MnO_2 (C_m), CB (C_b) and electrolyte (C_e) by the equation

$$1/C_p = 1/C_m + 1/C_b + 1/C_e. \quad (7)$$

This equivalent circuit model is chosen because alternate models, including the parallel model (with the MnO_2, CB and the electrolyte in parallel) and models with other parallel and series combinations (such as a model with MnO_2 in parallel with the series combination of CB and the electrolyte), do not give reasonable results, particularly when the resistivity is similarly modeled (Section 2.4). For example, the parallel model gives negative values of the CB resistivity. As in prior work [29], the same model is consistently used for both the dielectric behavior and the conduction behavior of the same material.

2.4. *Resistivity testing and analysis method*

The AC resistance is measured in the absence of an insulating film between the specimen and the copper contact (Fig. 3(a)). Other than this absence, the configuration is the same as that

Table 2 – Relative dielectric constant and resistivity of MnO_2–CB pastes and the CB part of the paste. CB = carbon black. Relative dielectric constant of MnO_2 = 101.5 ± 4.6, and resistivity of MnO_2 = 1921 ± 21 Ω cm, as obtained for the MnO_2 paste without CB (using the equivalent circuit in Fig. 2(c)) and considered to be unaffected by the CB addition. The pastes containing CB are analyzed using the equivalent circuit model in Fig. 2(d).

CB/MnO_2 mass ratio (%)	Volume fraction (%)			Relative dielectric constant		Resistivity (Ω cm)	
	MnO_2	CB	Electrolyte	Paste	CB	Paste	CB
0	82.7 ± 2.2	0	17.3 ± 1.4	103.2 ± 3.5	/	1589 ± 22	/
10.01 ± 0.01	64.6 ± 2.0	18.1 ± 0.9	17.3 ± 0.9	67.9 ± 1.8	29.4 ± 1.5	1251 ± 22	49.1 ± 2.3
15.01 ± 0.02	58.3 ± 1.8	24.5 ± 1.0	17.2 ± 0.9	64.1 ± 2.1	21.6 ± 1.1	1142 ± 36	33.6 ± 1.9

for relative dielectric constant measurement (Fig. 3(b)). The same RLC meter, AC voltage and frequencies are used. The frequency is 50 Hz.

The measured resistance R between the two copper contacts that sandwich the specimen includes the volume resistance R_s of the specimen and the resistance R_i of each of the two interfaces between the specimen and a copper contact, i.e.,

$$R = R_s + 2R_i. \tag{8}$$

By measuring R at three specimen thicknesses, the curve of R versus thickness is obtained (Fig. 1(a)). The intercept of this curve with the vertical axis equals $2R_i$, whereas the slope of this curve equals R_s/l, where R_s is the specimen resistance for the specimen thickness of l. The specimen resistivity is obtained by multiplying R_s/l by the specimen area A.

For an MnO_2 compact, the MnO_2, CB (if present) and air are considered as being in parallel (Fig. 2(a) and 2(b)), as explained in Section 2.3. The resistance of the compact R_c is thus related to the contributions by the MnO_2 (R_m) and the CB (R_b) by the equation

$$1/R_c = 1/R_m + 1/R_b. \tag{9}$$

By testing at three compact thicknesses, the compact resistivity ρ_c is obtained from the slope of the plot in Fig. 1(a). Based on Eq. (9), the resistivity ρ_c of the compact is given by

$$1/\rho_c = V_m/\rho_m + V_b/\rho_b, \tag{10}$$

where ρ_b is the resistivity of the CB in the paste. With ρ_c measured and ρ_m determined using Eq. (10) for the compact without CB ($V_b = 0$), ρ_b is obtained using Eq. (10). In other words, ρ_m is considered to be unaffected by the presence of the CB.

For the MnO_2 paste without CB, both the volume resistance R_m of the MnO_2 solid and the volume resistance R_e of the electrolyte contribute to the volume resistance R_p of the paste. With these contributors considered to be electrically in series (Fig. 2(c)),

$$R_p = R_m + R_e. \tag{11}$$

The quantity R_p is measured from a paste, using Eq. (8), with R_p substituting R_s. By testing at three paste thicknesses, the resistivity ρ_p is obtained from the slope of the plot in Fig. 1(a).

Based on Eq. (11), the resistivity of the paste (without CB) relates to those of the MnO_2 and electrolyte:

$$\rho_p = V_m\rho_m + (1 - V_m)\rho_e, \tag{12}$$

where ρ_m and ρ_e are the resistivities of the MnO_2 and electrolyte, respectively, and V_m is the volume fraction of MnO_2. Using Eq. (12), ρ_m is determined for the MnO_2 in the presence of the electrolyte.

For the MnO_2 paste with CB, the volume resistance R_m of the MnO_2, the resistance R_b of the CB and the volume resistance R_e of the electrolyte contribute to the volume resistance R_p of the paste. With these contributors considered to be electrically in series (Fig. 2(d)),

$$R_p = R_m + R_b + R_e. \tag{13}$$

The quantity R_p is measured. Based on Eq. (13), the resistivity of the paste (with CB) relates to those of the MnO_2, CB and electrolyte:

$$\rho_p = V_m\rho_m + V_b\rho_b + (1 - V_m - V_b)\rho_e, \tag{14}$$

where ρ_m, ρ_b and ρ_e are the resistivities of the MnO_2, CB and electrolyte, respectively, and V_m and V_b are the volume fractions of MnO_2 and CB respectively. Using Eq. (14), ρ_b is determined.

3. Results and discussion

Fig. 4(a) and (b) show representative plots akin to those in Fig. 1 for an MnO_2–CB compact; the plots are linear, as expected. Table 1 shows the measured values of the relative dielectric constant and electrical resistivity of the MnO_2 and MnO_2–CB compacts, along with the resulting calculated values for the MnO_2 solid and CB solid (if present) in the compact.

Fig. 5(a) and Table 1 show that the relative dielectric constant of the MnO_2–CB compact decreases with increasing CB volume fraction. This is due to the decreasing volume fraction and dielectric connectivity of the MnO_2 particles. Fig. 5(b) and Table 1 show that the relative dielectric constant of the CB in the MnO_2–CB compact decreases with increasing CB volume fraction, such that the value essentially levels off at CB contents exceeding 19 vol.%. This is due to the decreasing MnO_2 volume fraction and the consequent decreasing squishing of the CB; the squishing apparently enhances the polarizability of the CB, provided that the MnO_2 content exceeds 65 vol.% (corresponding to 19 vol.% CB, Table 1). In other words, the minimum MnO_2 content for squishing the CB to the extent of enhancing the CB polarizability is 65 vol.%.

In relation to the dry MnO_2 compacts (without CB), the resistivity of the MnO_2 compact decreases with increasing MnO_2 volume fraction (Fig. 6(a)), as expected due to the

Table 3 – Effect of the electrolyte on the properties of MnO_2 and CB in MnO_2–CB compact/paste. The compact corresponds to the case without electrolyte. The paste corresponds to the case with electrolyte.

	MnO_2		CB with CB/MnO_2 mass ratio = 10%		CB with CB/MnO_2 mass ratio = 15%	
	Relative dielectric constant	Resistivity (Ω cm)	Relative dielectric constant	Resistivity (Ω cm)	Relative dielectric constant	Resistivity (Ω cm)
Without electrolyte	68.1 ± 1.6	8790 ± 280	20.1 ± 1.2	200 ± 3	12.3 ± 0.7	165 ± 2
With electrolyte	101.5 ± 4.6	1921 ± 21	29.4 ± 1.5	49.1 ± 2.3	21.6 ± 1.1	33.6 ± 1.9

higher conductivity of MnO_2 compared to air. Using the equivalent circuit model in Fig. 2(a), the resistivity of the MnO_2 solid in the compact is obtained, as shown in Fig. 6(b)). The resistivity of the MnO_2 solid in the compact decreases with increasing MnO_2 volume fraction, such that it levels off at MnO_2 volume fractions exceeding 66% (Fig. 6(b)), due to (i) the increasing contact of the MnO_2 particles as the MnO_2 volume fraction increases and (ii) the presence of an upper limit for the degree of contact. In other words, the percolation threshold is about 66 vol.% MnO_2 for an MnO_2 compact without CB or the electrolyte.

The value of 65 vol.% mentioned above for the minimum MnO_2 content for squishing the CB to the extent of enhancing the CB polarizability is essentially equal to the percolation threshold of about 66 vol.% MnO_2 for an MnO_2 compact without CB or the electrolyte. This supports the notion that the squishing of the CB by the MnO_2 increases the dielectric connectivity of the CB, thereby enhancing the CB polarizability.

Fig. 5(c) and Table 1 show that the resistivity of the MnO_2–CB compact decreases with increasing CB volume fraction. This is due to the high conductivity of CB. Fig. 5(d) and Table 1 show that the resistivity of the CB in the MnO_2–CB compact decreases with increasing CB volume fraction. This is due to the decreasing MnO_2 volume fraction and the consequent increasing volume fraction and conduction connectivity of the CB particles. The CB resistivity does not level off as the CB volume fraction increases (Fig. 5(d)), suggesting that CB conduction percolation has not been attained, even at the highest CB volume fraction studied (30%).

Table 2 shows that the relative dielectric constant of the paste decreases with increasing CB volume fraction (i.e., decreasing MnO_2 volume fraction), as expected due to the high value of the relative dielectric constant of MnO_2 (101.5 ± 4.6, Table 3). The resistivity of the paste decreases with increasing CB volume fraction, as expected due to the high conductivity of CB. The relative dielectric constant of the CB in the paste decreases with increasing CB content, while the resistivity of the CB decreases with increasing CB content. The decrease in resistivity of CB is attributed to the increased conduction connectivity of the CB as the CB content increases. The decrease in the relative dielectric constant of CB is attributed to the decreasing squishing of the CB as the MnO_2 content decreases. The squishing apparently helps the polarization of the CB, as explained above for the case without the electrolyte.

Table 3 also shows the resistivity of CB is significantly decreased by the presence of the electrolyte, whether the CB/MnO_2 mass ratio is 10% or 15%. This means that the electrolyte helps the conduction connectivity of the CB particles. Table 3 also shows that the relative dielectric constant of CB is increased by the presence of the electrolyte, irrespective of the CB/MnO_2 mass ratio. This means that the electrolyte helps the dielectric connectivity of the CB particles, so that the excursion of the charges responsible for the polarization can be larger.

Table 4 shows that, in the presence of the electrolyte, the resistivity of CB increases with increasing MnO_2 volume fraction from 0% to 65%. This is because the increasing MnO_2 volume fraction and the accompanying decreasing CB volume fraction cause less conduction connectivity of the CB

Table 4 – Effect of MnO_2 on the properties of CB in the presence of the electrolyte.

MnO_2 volume fraction (%)	CB	
	Relative dielectric constant	Resistivity (Ω cm)
0	31.2 ± 1.3*	12.5 ± 0.3*
58.3 ± 1.8	21.6 ± 1.1	33.6 ± 1.9
64.6 ± 2.0	29.4 ± 1.5	49.1 ± 2.3

* From [29].

particles. The higher value of the relative dielectric constant of CB in the absence of MnO_2 compared to that in the presence of MnO_2 and the consequent apparent anomaly in the trend associated with the effect of the MnO_2 volume fraction on the relative dielectric constant in Table 4 probably relates to (i) the greater connectivity of the CB particles in the absence of MnO_2 and (ii) the increasing squishing of CB as the MnO_2 content increases (Table 5).

The resistivity of CB is lower in an MnO_2 paste (34–49 Ω cm, Table 2) than in an MnO_2 compact (165–236 Ω cm, Table 1). This is due to the electrolyte enhancing the conduction connectivity of the CB particles and is consistent with the result that the resistivity of MnO_2 is decreased in the presence of the electrolyte (Table 3). These values of the CB resistivity are all higher than the value of 13 Ω cm [29] for CB in the absence of both MnO_2 and the electrolyte, indicating that the conduction connectivity of CB is exceptionally high in the absence of MnO_2.

For the paste containing 65 vol.% MnO_2, 18 vol.% CB and 17 vol.% electrolyte (Table 2), the MnO_2, CB and electrolyte contribute 99.2%, 0.71% and 0.053% respectively to the paste resistivity. This means that the electrolyte rather than CB dominates the conduction in this paste.

The CB contributes electronic conductivity, whereas the electrolyte contributes ionic conductivity, with the paste being a mixed conductor that is dominated by ionic conduction. The AC testing method (50 Hz) used in this work is sensitive to both ionic conduction and electronic conduction, such that the two types of conduction cannot be distinguished. For the function of an electrode in an electrochemical cell, the electrode must be an electronic conductor. Therefore, in spite of the fact that the electronic conduction provided by the CB is minor compared to the ionic conduction provided by the electrolyte, the CB contribution is critical for electrode performance.

The value of the MnO_2 resistivity (8790 ± 280 Ω cm in the absence of the electrolyte (Table 3) is higher than the value of 5900 Ω cm previously reported for MnO_2 at a relative humidity of 85% [30] and attributed to proton conduction under high humidity [30,31]. Since the MnO_2 in the paste of this work is immersed in an aqueous solution containing protons from the acid, its resistivity (1921 ± 21 Ω cm in the presence of the electrolyte, Table 3) being lower than the value (5900 Ω cm) at a relative humidity of 85% is consistent with the notion of proton conduction.

4. Conclusion

The relative dielectric constant and electrical conductivity (50 Hz) of electrochemical electrodes with MnO_2 particles mixed with CB (conductive additive at a minor proportion), with and without electrolyte (15 vol.% sulfuric acid) permeation, are reported, with unprecedented decoupling of the MnO_2, CB and electrolyte/air contributions and unprecedented determination of the decoupled CB properties. The rigor of the approach is enabled by the decoupling of the volumetric (electrode) and interfacial (interface between electrode and electrical contact) contributions. This work is an extension of prior work on CB without MnO_2 [29].

The resistivity of CB is significantly decreased and the relative dielectric constant of CB is increased by the presence of the electrolyte. This means that the electrolyte helps the conduction/dielectric connectivity of the CB particles. The values of the CB resistivity in the presence of MnO_2 are all higher than the value of 13 Ω cm [29] for CB in the absence of MnO_2, indicating that the conduction connectivity of CB is reduced by the presence of MnO_2.

The resistivity of CB in an MnO_2 compact decreases from 236 to 165 Ω cm (without leveling off) as the CB volume

Table 5 – Relative dielectric constant and electrical resistivity of the MnO_2 paste (without CB) and the MnO_2 solid in the paste. The values for the solid are obtained by modeling the paste as the solid and the electrolyte in series electrically (Fig. 2(c)). The addition of the electrolyte to MnO_2 significantly decreases the resistivity, but increases the relative dielectric constant only slightly.

MnO_2 volume fraction (%)	Relative dielectric constant		Resistivity (Ω cm)	
	Paste	MnO_2 solid	Paste	MnO_2 solid
29.7 ± 0.6*	87.7 ± 1.4	67.1 ± 2.2	465 ± 7	1568 ± 34
30.9 ± 0.9*	88.8 ± 1.4	69.7 ± 3.3	632 ± 8	2022 ± 36
31.4 ± 0.9*	90.5 ± 1.7	70.7 ± 3.4	705 ± 10	2145 ± 51
82.7 ± 2.2[a]	103.2 ± 3.5	101.5 ± 4.6	1589 ± 22	1921 ± 21

* Obtained with heating the paste in order to evaporate away a part of the electrolyte in the paste.
[a] Obtained without heating the paste.

fraction increases from 13.5% to 29.5% and the corresponding MnO_2 volume fraction decreases from 68.6% to 58.7%, indicating increasing degree of conduction connectivity of the CB, such that conduction percolation has not been reached. This is accompanied by decrease of the relative dielectric constant of CB from 53 to 12, suggesting decreasing polarizability of the CB as the CB is less squished by the lower volume fraction of MnO_2. This trend of decreasing polarizability levels off when the MnO_2 content decreases to below 65 vol.%, implying that the minimum MnO_2 content for squishing the CB to the extent of enhancing the CB polarizability is 65 vol.%. For similar reasons, the resistivity of CB in the MnO_2 paste decreases from 49 to 34 Ω cm and the relative dielectric constant of the CB decreases from 29 to 22 as the CB volume fraction increases from 18% to 25%.

Acknowledgement

The authors are grateful to Dr. Andi Wang of University at Buffalo, State University of New York, for technical assistance.

Appendix A. Supplementary data

Supplementary data associated with this article can be found, in the online version, at http://dx.doi.org/10.1016/j.carbon.2015.04.047.

REFERENCES

[1] Zhang Y, Xue D. Recent advances in MnO_2: chemical synthesis and supercapacitance. Mater Focus 2013;2(3):161–73.
[2] Whittingham MS, Zavalij PY. Manganese dioxides as cathodes for lithium rechargeable cells: the stability challenge. Solid State Ionics 2000;131(1,2):109–15.
[3] Frysz CA, Shui X, Chung DDL. Carbon filaments and carbon black as a conductive additive to the manganese dioxide cathode of a lithium electrolytic cell. J Power Sources 1996;58(1):41–54.
[4] Xu C, Kang F, Li B, Du H. Recent progress on manganese dioxide based supercapacitors. J Mater Res 2010;25(8):1421–32.
[5] Ran F, Fan H, Wang L, Zhao L, Tan Y, Zhang X, et al. A bird nest-like manganese dioxide and its application as electrode in supercapacitors. J Energy Chem 2013;22(6):928–34.
[6] Tadjer MJ, Mastro MA, Rojo JM, Mojena AB, Calle F, Kub FJ, et al. MnO_2-based electrochemical supercapacitors on flexible carbon substrates. J Electron Mater 2014;43(4):1188–93.
[7] Sahu V, Shekhar S, Ahuja P, Gupta G, Singh SK, Sharma RK, et al. Synthesis of hydrophilic carbon black; role of hydrophilicity in maintaining the hydration level and protonic conduction. RSC Adv 2013;3(12):3917–24.
[8] Kim M, Yoo M, Yoo Y, Kim J. Capacitance behavior of composites for supercapacitor applications prepared with different durations of graphene/nanoneedle MnO_2 reduction. Microelectron Reliab 2014;54(3):587–94.
[9] Sen P, De A, Chowdhury AD, Bandyopadhyay SK, Agnihotri N, Mukherjee M. Conducting polymer based manganese dioxide nanocomposite as supercapacitor. Electrochim Acta 2013;108:265–73.
[10] Kang J, Chen L, Hou Y, Li C, Fujita T, Lang X, et al. Electroplated thick manganese oxide films with ultrahigh capacitance. Adv Energy Mater 2013;3(7):857–63.
[11] Sidhu NK, Rastogi AC. Nanoscale blended MnO_2 nanoparticles in electro-polymerized polypyrrole conducting polymer for energy storage in supercapacitors. MRS Online Proceedings Library 1552 [Nanostructured Metal Oxides for Advanced Applications] opl.2013.667, 6 pp. (2013). DOI: 10.1557/opl.2013.667.
[12] Wang H, Peng C, Zheng J, Peng F, Yu H. Design, synthesis and the electrochemical performance of MnO_2/C@CNT as supercapacitor material. Mater Res Bull 2013;48(9):3389–93.
[13] Ranjusha R, Prathibha V, Ramakrishna S, Nair AS, Anjali P, Subramanian KRV, et al. Conductive blends of camphoric carbon nanobeads anchored with MnO_2 for high-performance rechargeable electrodes in battery/supercapacitor applications. Scripta Mater 2013;68(11):881–4.
[14] Lin J, Zheng Y, Du Q, He M, Deng Z. Synthesis and electrochemical properties of graphene/MnO_2/conducting polymer ternary composite for supercapacitors. NANO 2013;8(1). 1350004/1–1350004/8.
[15] Zheng Y, Du Q, He M, Deng Z, Liu X. Synthesis and electrochemical properties of graphite oxide/MnO_2/conducting polymer ternary composite for supercapacitors. Micro Nano Lett 2012;7(8):778–81. http://dx.doi.org/10.1049/mnl.2012.0405.
[16] Gambou-Bosca A, Belanger D. Effect of the formulation of the electrode on the pore texture and electrochemical performance of the manganese dioxide-based electrode for application in a hybrid electrochemical capacitor. J Mater Chem A 2014;2(18):6463–73.
[17] Kim K, Park S. Electrochemical performance of activated carbons/Mn_3O_4-carbon blacks for supercapacitor electrodes. Bull Korean Chem Soc 2013;34(8):2343–7.
[18] Zolfaghari A, Naderi HR, Mortaheb HR. Carbon black/manganese dioxide composites synthesized by sonochemistry method for electrochemical supercapacitors. J Electroanal Chem 2013;697:60–7.
[19] Kai K, Kobayashi Y, Yamada Y, Miyazaki K, Abe T, Uchimoto Y, et al. Electrochemical characterization of single-layer MnO_2 nanosheets as a high-capacitance pseudocapacitor electrode. J Materials Chem 2012;22(29):14691–5.
[20] Jacob GM, Yang QM, Zhitomirsky I. Electrodes for electrochemical supercapacitors. Mater Manuf Processes 2009;24(12):1359–64.
[21] Shimamoto K, Tadanaga K, Tatsumisago M. All-solid-state electrochemical capacitors using MnO_2 electrode/SiO_2-Nafion electrolyte composite prepared by the sol–gel process. J Power Sources 2014;248:396–9.
[22] Zhang J, Zhao XS. A comparative study of electrocapacitive properties of manganese dioxide clusters dispersed on different carbons. Carbon 2013;52:1–9.
[23] Liu Y, Yan D, Li Y, Wu Z, Zhuo R, Li S, et al. Manganese dioxide nanosheet arrays grown on graphene oxide as an advanced electrode material for supercapacitors. Electrochim Acta 2014;117:528–33.
[24] Yang W, Gao Z, Wang J, Wang B, Liu Q, Li Z, et al. Synthesis of reduced graphene nanosheet/urchin-like manganese dioxide composite and high performance as supercapacitor electrode. Electrochim Acta 2012;69:112–9.
[25] Jiang R, Cui C, Ma H. Using graphene nanosheets as a conductive additive to enhance the capacitive performance of α-MnO_2. Electrochim Acta 2013;104:198–207.
[26] Zamri MFMA, Zein SHS, Abdullah AZ, Basir NI. The optimization of electrical conductivity using central composite design for polyvinyl alcohol/multiwalled carbon

nanotube-manganese dioxide nanofiber composites synthesised by electrospinning. J Appl Sci 2012; 12(4):345–53.
[27] Higgins TM, McAteer D, Coelho JCM, Sanchez BM, Gholamvand Z, Moriarty G, et al. Effect of percolation on the capacitance of supercapacitor electrodes prepared from composites of manganese dioxide nanoplatelets and carbon nanotubes. ACS Nano 2014;8(9):9567–79.
[28] Lu W, Chung DDL. A comparative study of carbons for use as an electrically conducting additive in the manganese dioxide cathode of an electrochemical cell. Carbon 2002;40(ER3):447–9.
[29] Wang A, Chung DDL. Dielectric and electrical conduction behavior of carbon paste electrochemical electrodes, with decoupling of carbon, electrolyte and interface contributions. Carbon 2014;72:135–51.
[30] Ueda Y, Tokuda Y, Yoko T, Takeuchi K, Kolesnikov AI, Koyanaka H. Electrochemical property of proton-conductive manganese dioxide for sensoring hydrogen gas concentration. Solid State Ionics 2012;225:282–5.
[31] Koyanaka H, Ueda Y, Takeuchi K, Kolesnikov AI. Effect of crystal structure of manganese dioxide on response for electrolyte of a hydrogen sensor operative at room temperature. Sens Actuator B 2013;183:641–7.